Supplement

Solid-state ^{13}C-NMR spectroscopic determination of sidechain mobilities in zirconium-based metal-organic frameworks

Günter Hempel,[1] Ricardo Kurz,[1] Silvia Paasch,[2] Kay Saalwächter,[1] and Eike Brunner[2]

[1] *Martin-Luther-Universität Halle-Wittenberg, Institut für Physik – NMR,*
Betty-Heimann-Str. 7, 06120 Halle, Germany
[2] *Technische Universität Dresden, Fakultät für Chemie und Lebensmittelchemie,*
Bioanalytische Chemie, 01062 Dresden, Germany

S1.   LINE DECOMPOSITIONS

See Figs. 1, 2, and 3.

S2.   DIPSHIFT DIAGRAMS

In the diagrams in this section, at the left-hand side the data are shown together with the fitted model functions. The right-hand sides show plots of the mean-square deviation χ^2 versus damping constant r and residual dipolar coupling D_{res}. In the latter, the cross marks the position of minimum mean-square deviation χ^2_{min}; the closed line connects all points where $\chi^2 = 2\chi^2_{\mathrm{min}}$. The evaluation was not executed for all spinning frequencies; it was omitted for such frequencies where the line under consideration had a distance of an integer multiple of spinning frequency to another line.
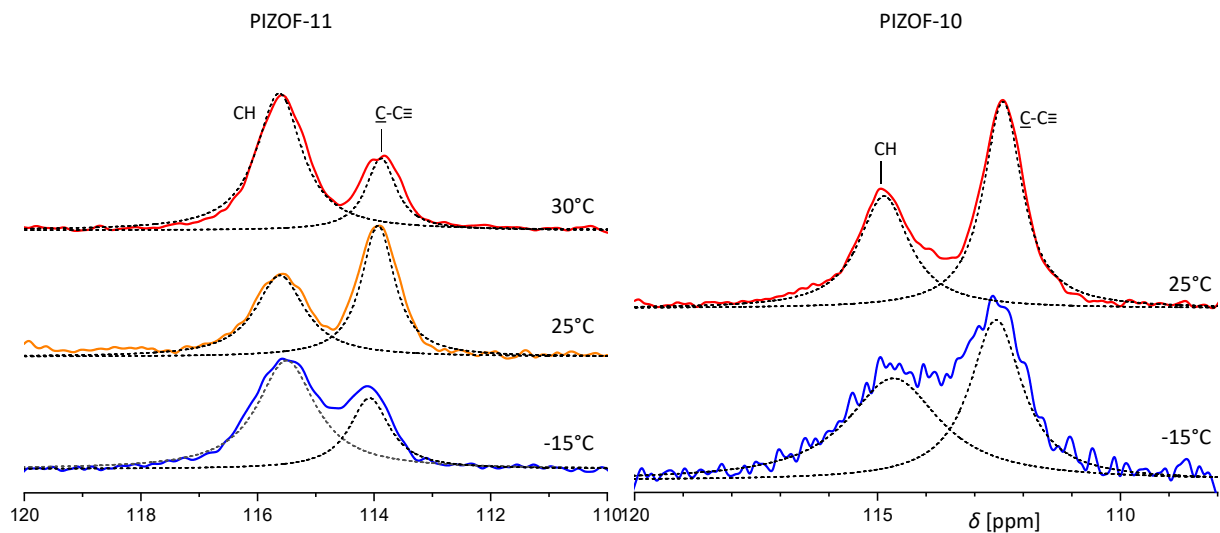
Figure 1. Decomposition of overlapping middle-ring lines of both protonated carbons and those carbons bound to C≡C in PIZOF-10 (right) and in PIZOF-11 (left).)
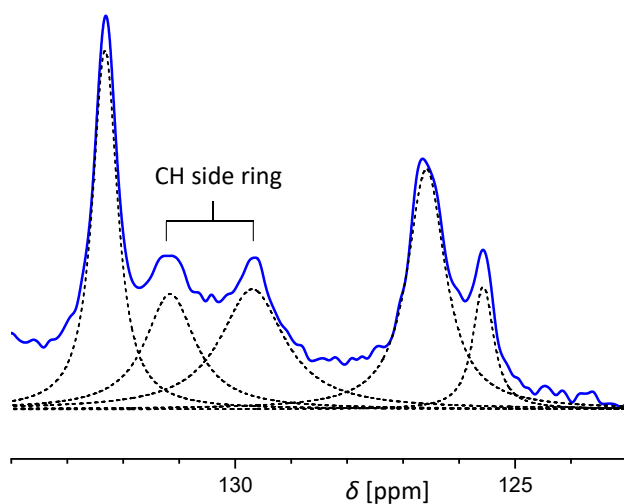

Figure 2. Decomposition of overlapping lines in the region 120 ... 140 ppm in PIZOF-2.)
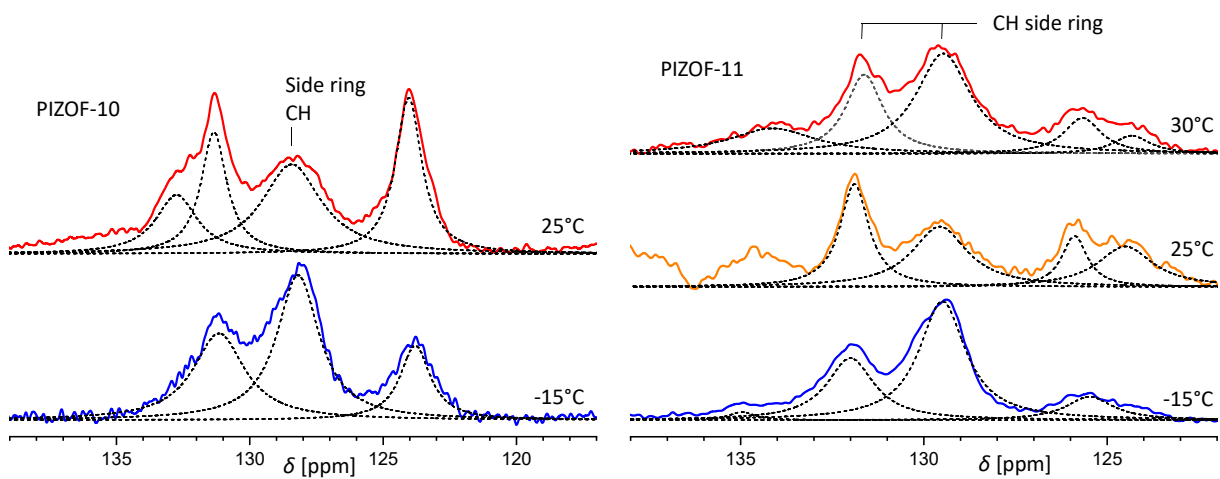

Figure 3. Decomposition of overlapping lines in the region 120 ... 140 ppm in PIZOF-10 and in PIZOF-11.)
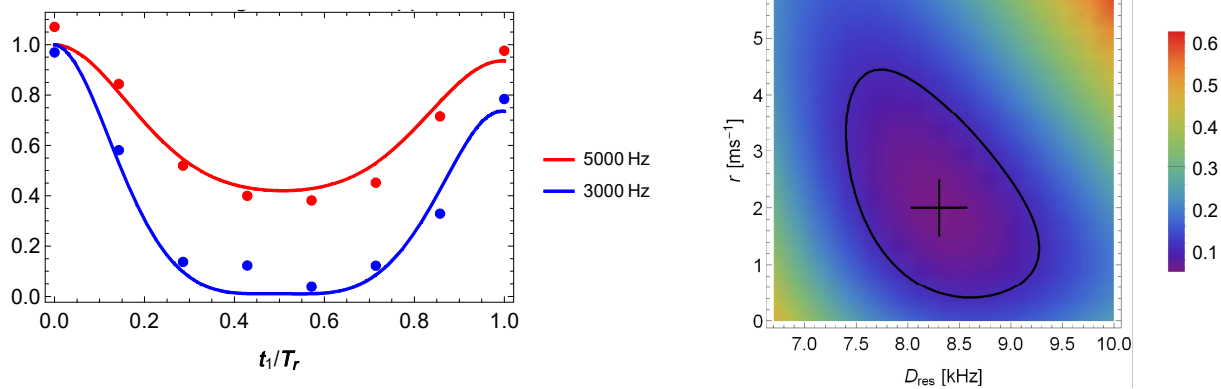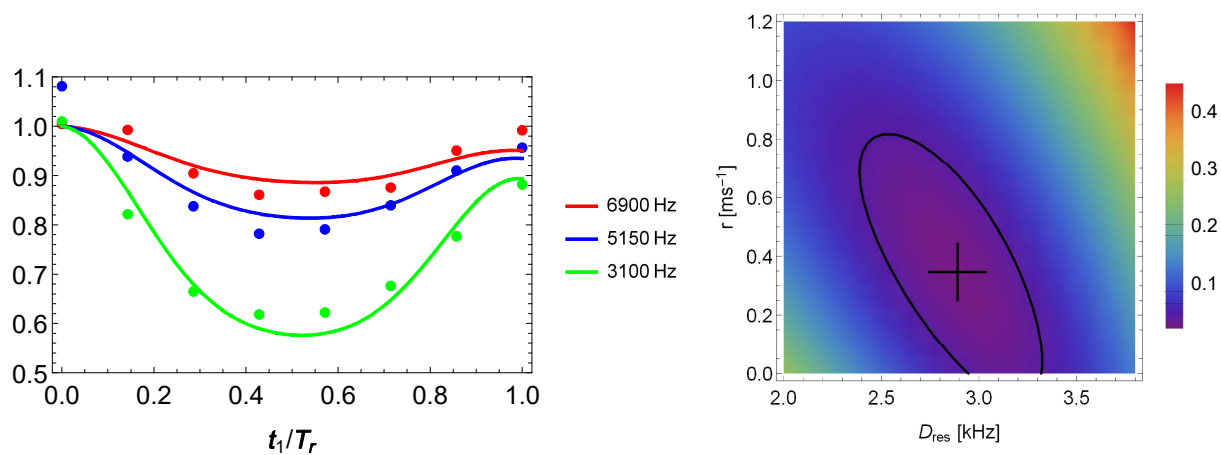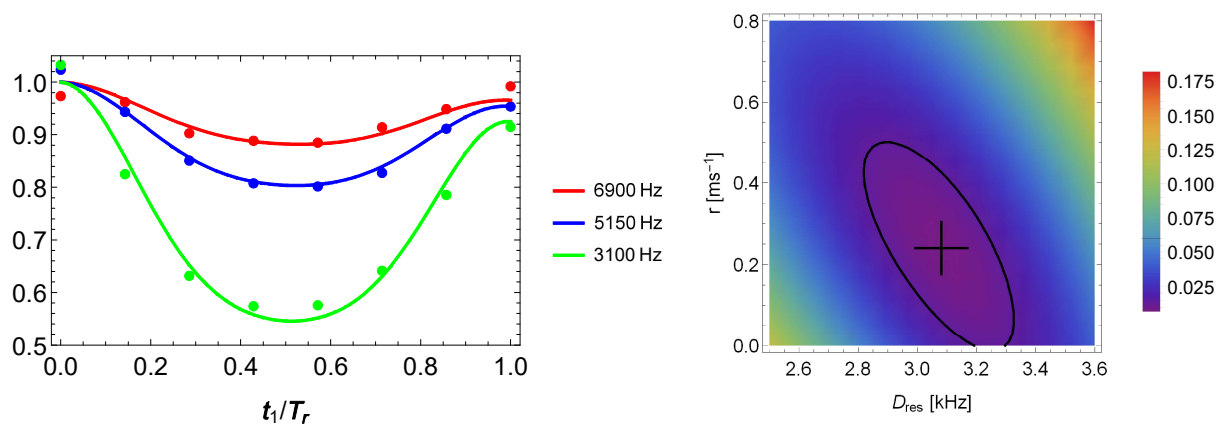
Figure 4. PIZOF-2, -15°C, CH of side ring, model function 1

Figure 5. PIZOF-10, -15°C, CH$_2$, left component, model function 3

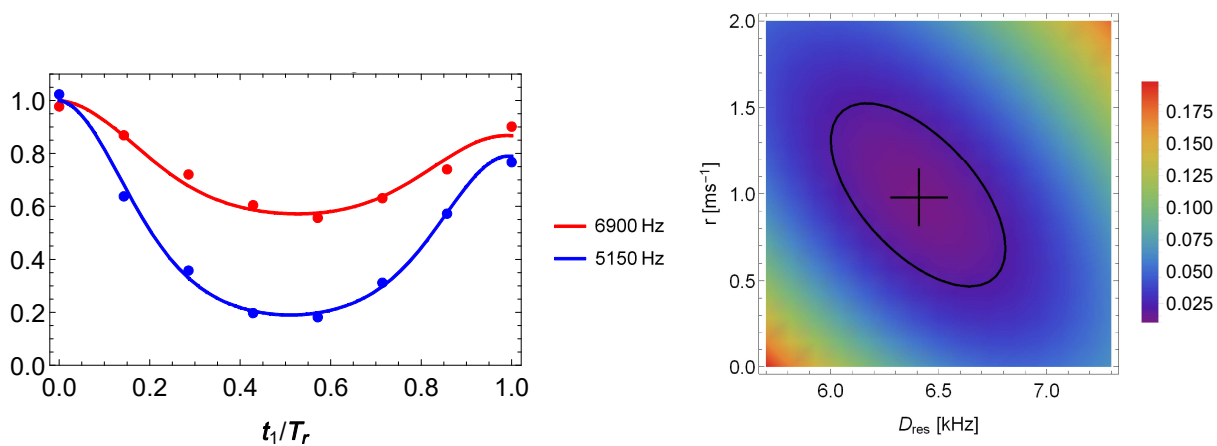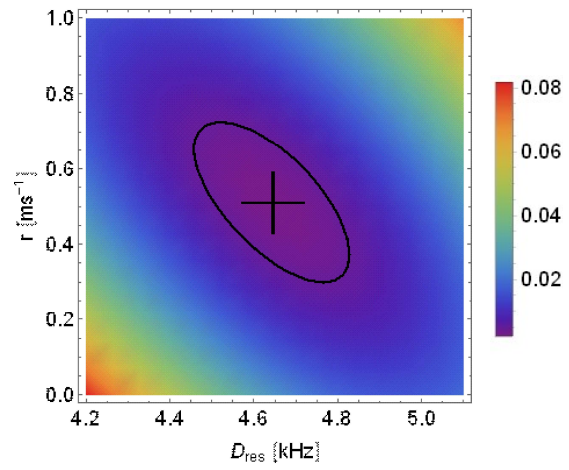Figure 6. PIZOF-10, -15°C, CH$_2$, middle component, model function 3
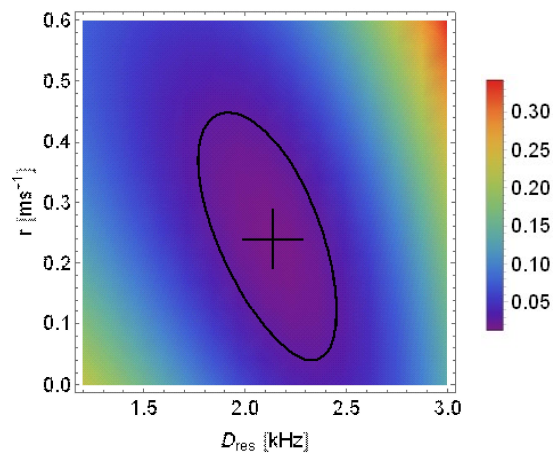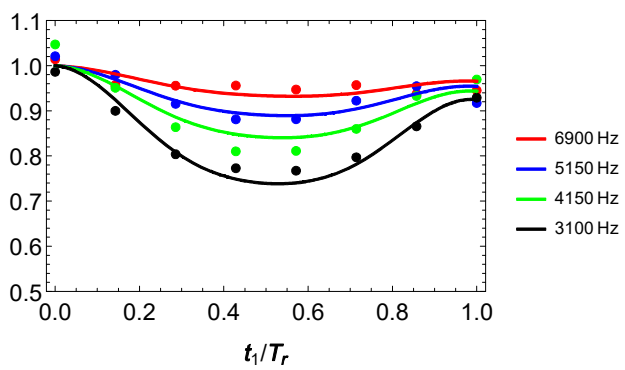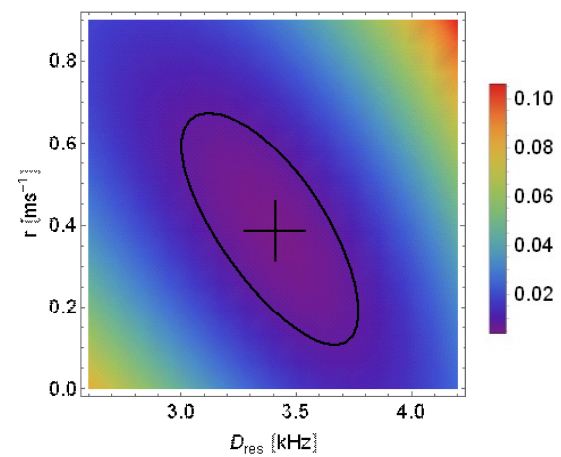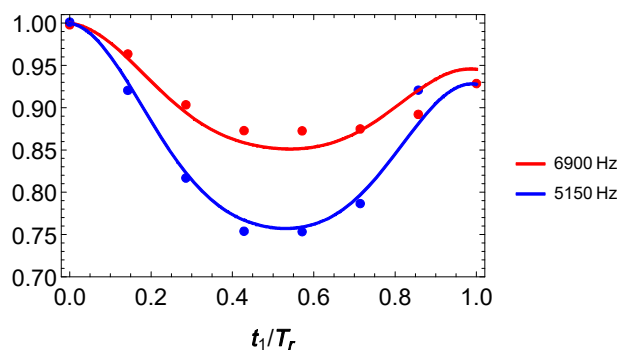
Figure 7. PIZOF-10, -15°C, CH$_2$, right component, model function 3

Figure 8. PIZOF-10, -15°C, CH of side ring, model function 1

Figure 9. PIZOF-10, 25°C, CH$_2$ right component, model function 3

Figure 10. PIZOF-10, 25°C, CH$_2$ 2nd component from right, model function 3

Figure 11. PIZOF-10, 25°C, CH$_2$ middle component, model function 3

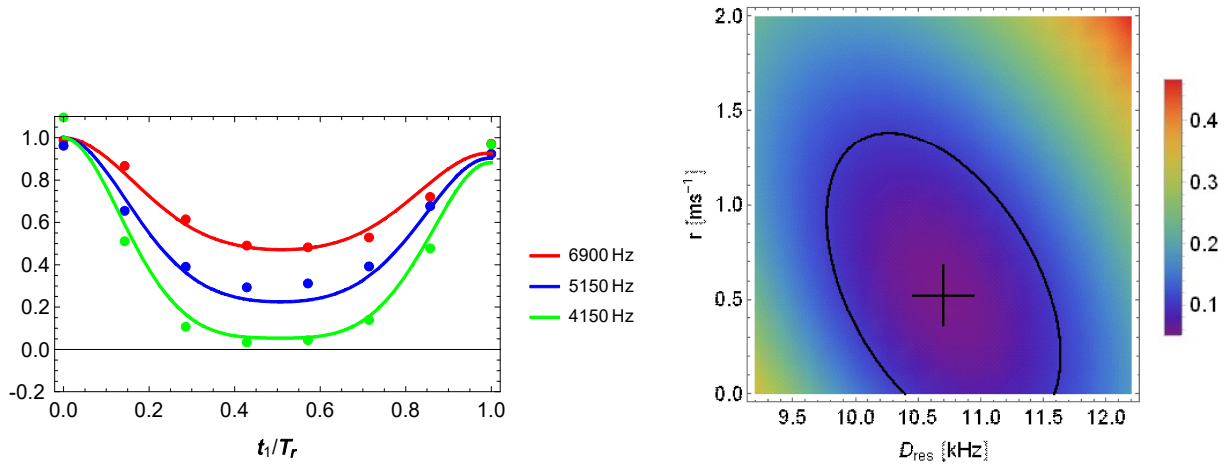Figure 12. PIZOF-10, 25°C, CH$_2$ 2nd component from right, model function 3

Figure 13. PIZOF-10, 25°C, CH of middle ring, model function 1
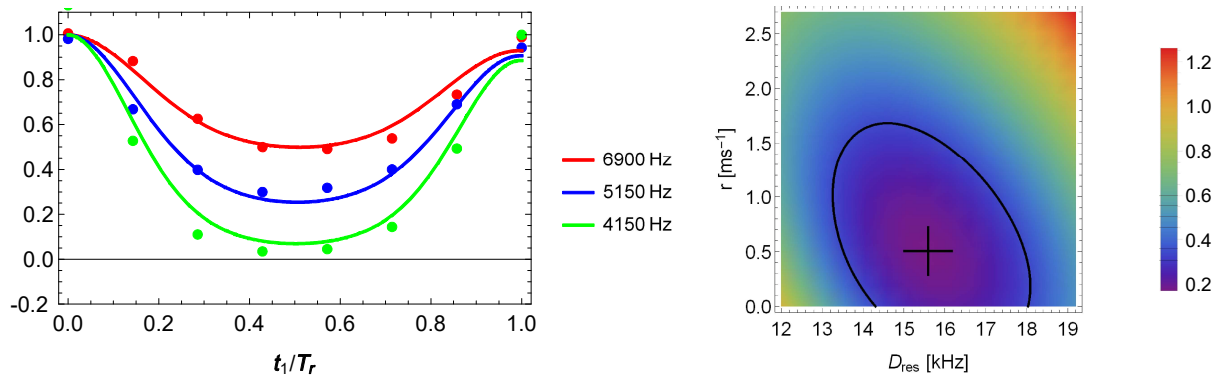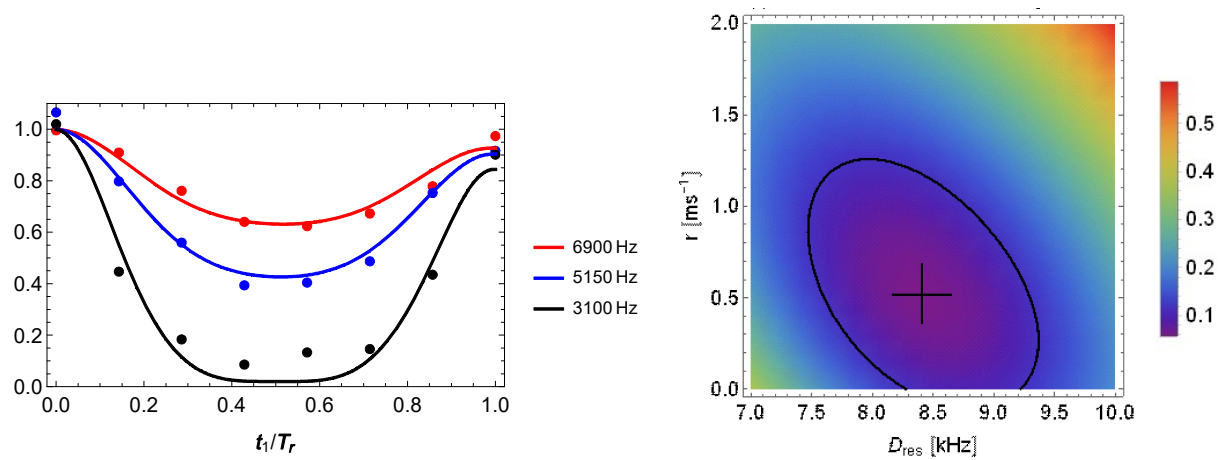

Figure 14. PIZOF-10, 25°C, CH of middle ring, model function 2

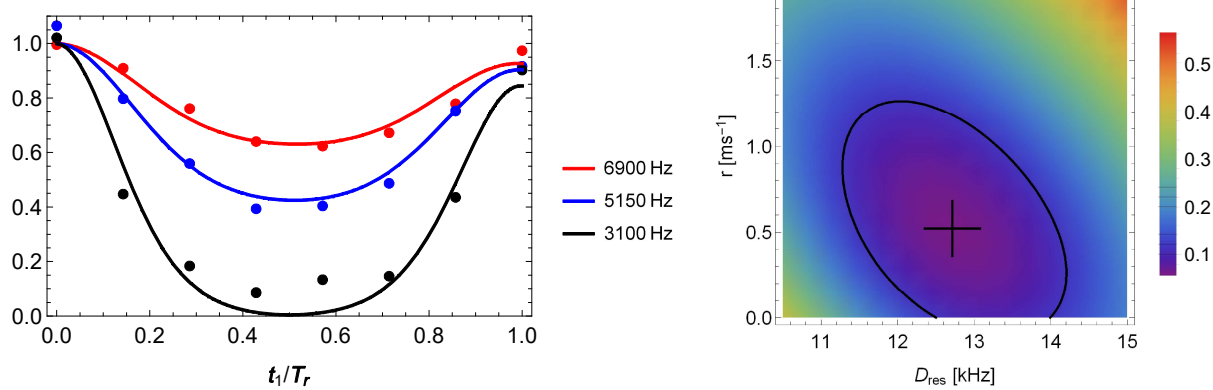Figure 15. PIZOF-10, 25°C, CH of side ring, model function 1

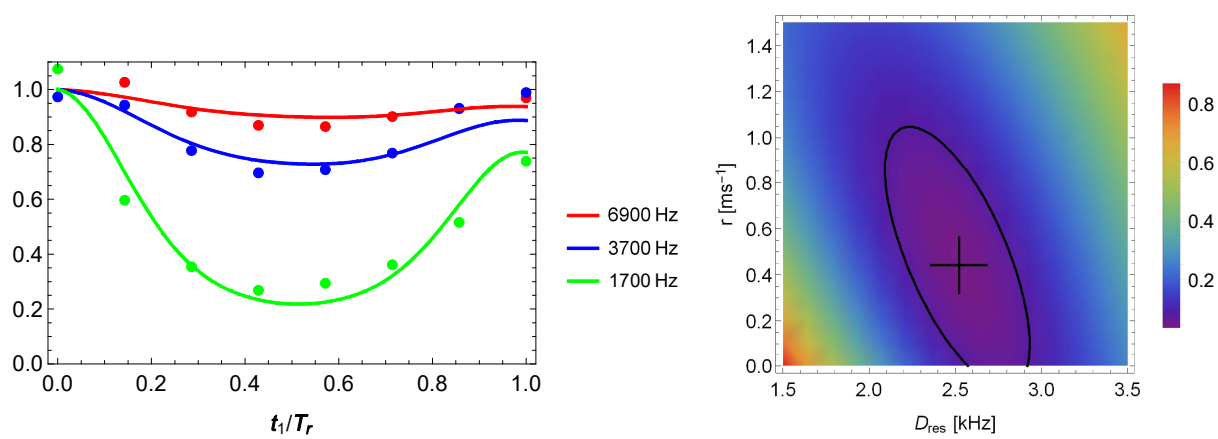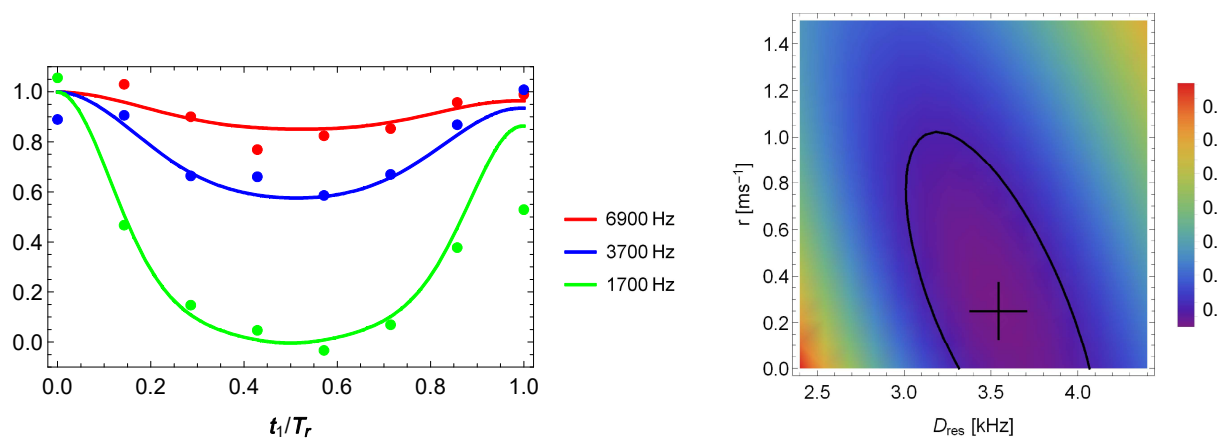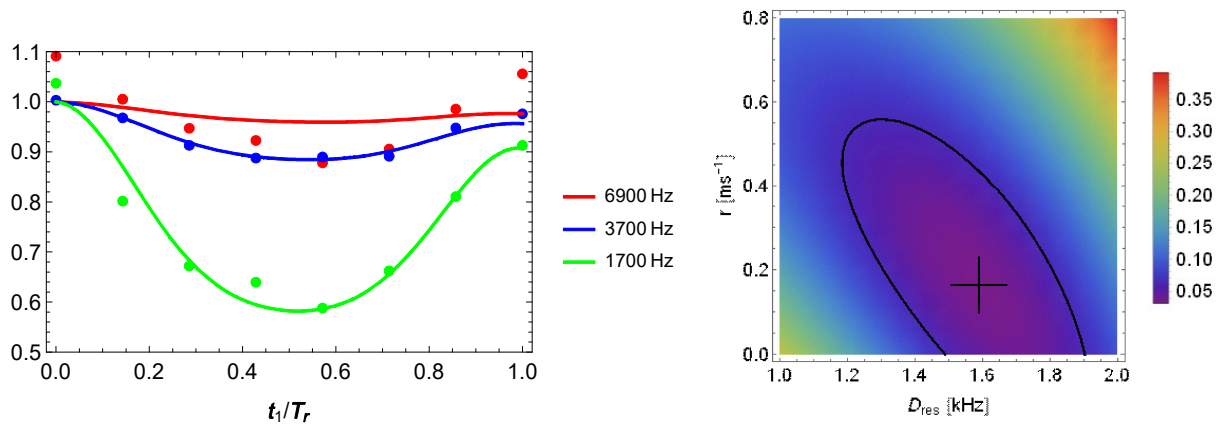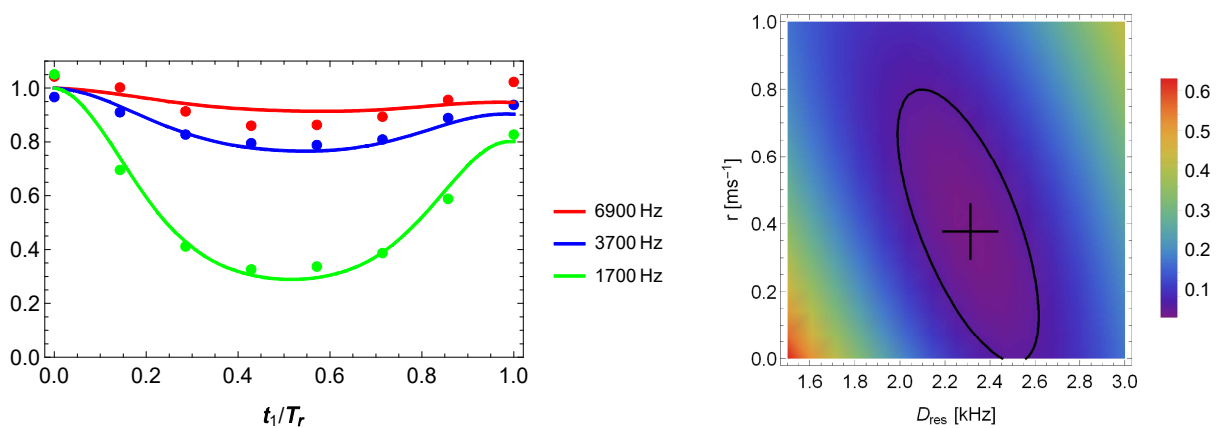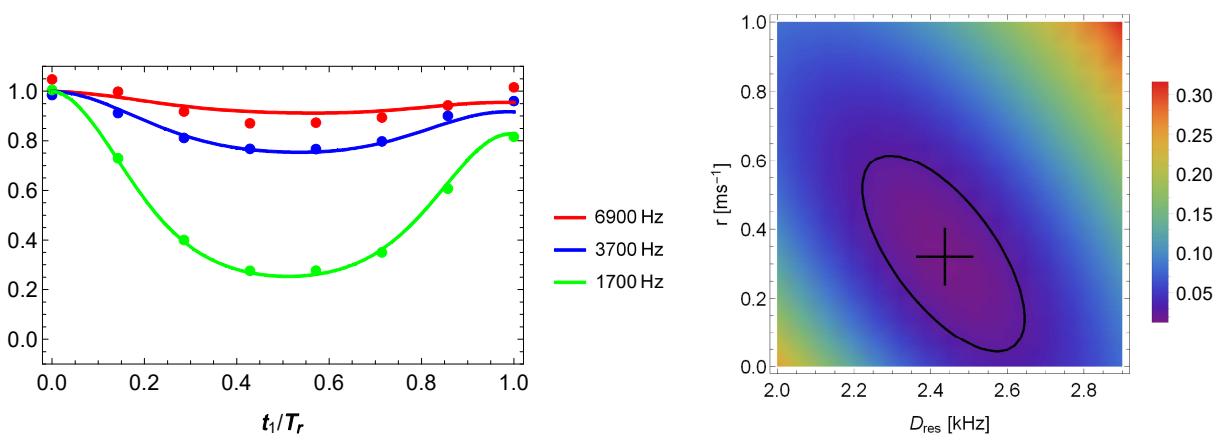Figure 16. PIZOF-10, 25°C, CH of side ring, model function 2

Figure 17. PIZOF-11, -15°C, δ-CH$_2$ left component, model function 3

Figure 18. PIZOF-11, -15°C, ε-CH$_2$, model function 3

Figure 19. PIZOF-11, 30°C, γ-CH$_2$, model function 3

Figure 20. PIZOF-11, 30°C, δ-CH$_2$, model function 3

Figure 21. PIZOF-11, 30°C, ε-CH$_2$, model function 3
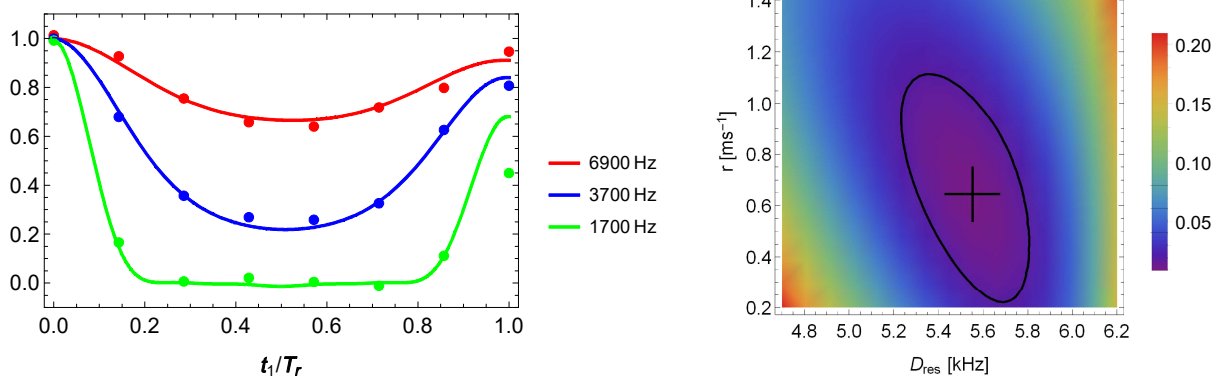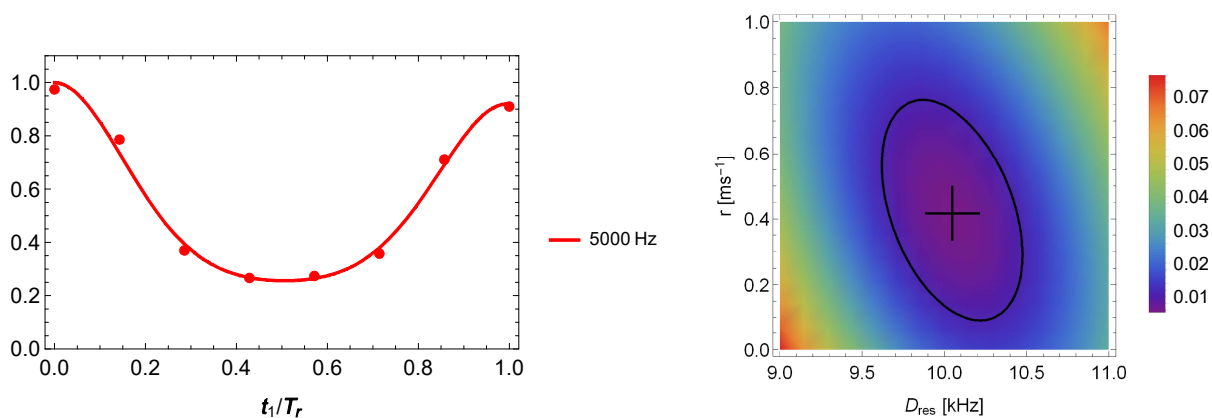
Figure 22. PIZOF-11, 30°C, ω-CH$_2$, model function 3
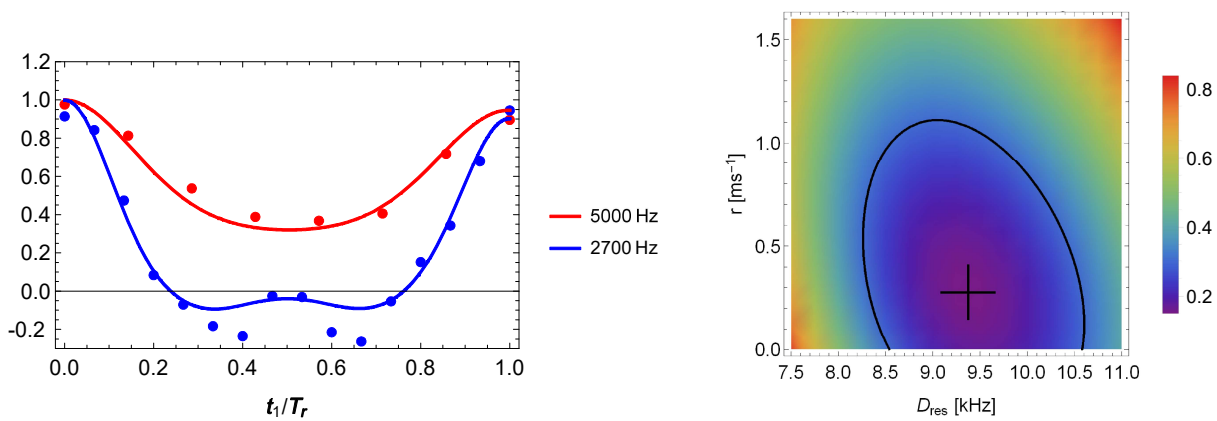

Figure 23. PIZOF-11, 25°C, middle ring, model function 1

Figure 24. PIZOF-11, 25°C, side ring, model function 1